# An Extensive Analysis on the Underlying Premises Behind Deep Reinforcement Learning Algorithm Design

**Anonymous authors**
Paper under double-blind review

## Abstract

The progress in reinforcement learning algorithm development is at one of its highest points starting from the initial study that enabled sequential decision making from high-dimensional observations. Currently, deep reinforcement learning research has had quite recent breakthroughs from learning without the presence of rewards to learning functioning policies without even knowing the rules of the game. In our paper we focus on the underlying premises that are actively used in deep reinforcement learning algorithm development. We theoretically demonstrate that the performance profiles of the algorithms developed for the data-abundant regime do not transfer to the data-limited regime monotonically. We conduct large-scale experiments in the Arcade Learning Environment and our results demonstrate that the baseline algorithms perform significantly better in the data-limited regime compared to the set of algorithms that were initially designed and compared in the data-abundant regime.

## 1 Introduction

Reinforcement learning research achieved high acceleration upon the proposal of the initial study on approximating the state-action value function via deep neural networks (Mnih et al., 2015). Following this initial study several different highly successful deep reinforcement learning algorithms have been proposed (Hasselt et al., 2016b; Wang et al., 2016; Hessel et al., 2018; 2021) from focusing on different architectural ideas to employing estimators targeting overestimation, all of which were designed and tested in the high-data regime (i.e. two hundred million frame training).

An alternative recent line of research with an extensive amount of publications focused on pushing the performance bounds of deep reinforcement learning policies in the low-data regime (Yarats et al., 2021; Ye et al., 2021; Kaiser et al., 2020; van Hasselt et al., 2019; Kielak, 2019) (i.e. with one hundred thousand environment interaction training). Several different unique ideas in current reinforcement learning research, from model-based reinforcement learning to increasing sample efficiency with observation regularization, gained acceleration in several research directions based on policy performance comparisons demonstrated in the Arcade Learning Environment 100K benchmark. In this paper, we demonstrate that there is a significant overlooked underlying premise driving this line of research without being explicitly discussed: that the performance profiles of deep reinforcement learning algorithms have a monotonic relationship with different sample-complexity regions. This implicit assumption, that is commonly shared amongst a large collection of low-data regime studies, carries a significant importance due to the fact that these studies shape future research directions with incorrect reasoning while influencing the overall research efforts put in for particular research ideas for several years following. Thus, in our paper we target these underlying premises and aim to answer the following questions:

- *How can we theoretically explain the relationship between asymptotic sample complexity versus the low-data regime sample complexity in deep reinforcement learning?*
- *How would the performance profiles of deep reinforcement learning algorithms designed for the high-data regime transform to the low-data regime?*
- *Can we expect the performance rank of algorithms to hold with variations on the number of samples used in policy training?*

Hence, to be able to answer the questions raised above in our paper we focus on sample complexity in deep reinforcement learning and make the following contributions:

- We provide theoretical foundation on the non-transferability of the performance profiles of deep reinforcement learning algorithms designed for the high-data regime to the low-data regime.
- We theoretically demonstrate that the performance profile has a non-monotonic relationship with the asymptotic sample complexity and the low-data sample complexity region. Furthermore, regarding the central focus of the large scale implicit assumption instances, we prove that the sample complexity of the algorithm family that learns the state-action value distribution is higher than the sample complexity of baseline deep $\mathcal{Q}$-network algorithms.
- We conduct large scale extensive experiments for a variety of deep reinforcement learning baseline algorithms in both the low-data regime and the high-data regime Arcade Learning Environment benchmark.
- We highlight that recent algorithms proposed and evaluated in the Arcade Learning Environment 100K benchmark are significantly affected by the implicit assumption on the relationship between performance profiles and sample complexity.

## 2 Background and Preliminaries

The reinforcement learning problem is formalized as a Markov Decision Process (MDP) represented as a tuple $\langle S, A, \mathcal{P}, \mathcal{R}, \gamma, \rho_0 \rangle$ where $S$ represents the state space, $A$ represents the set of actions, $\mathcal{P} : S \times A \to \Delta(S)$ represents the transition probability kernel that maps a state and an action pair to a distribution on states, $\mathcal{R} : S \times A \to \mathbb{R}$ represents the reward function, and $\gamma \in (0, 1]$ represents the discount factor. The aim in reinforcement learning is to learn an optimal policy $\pi(s, a)$ that outputs the probability of taking action $a$ in state $s$, $\pi : S \times A \to \mathbb{R}$ that will maximize expected cumulative discounted rewards $R = \mathbb{E}_{a_t \sim \pi(s_t, \cdot), s_{t+1} \sim \mathcal{P}(\cdot|s_t, a_t)} \sum_t \gamma^t \mathcal{R}(s_t, a_t, s_{t+1})$. This objective is achieved by constructing a state-action value function that learns for each state-action pair the expected cumulative discounted rewards that will be obtained if action $a \in A$ is executed in state $s \in S$.

$$\mathcal{Q}(s_t, a_t) = \mathcal{R}(s_t, a_t, s_{t+1}) + \gamma \sum_{s_t} \mathcal{P}(s_{t+1}|s_t, a_t) \mathcal{V}(s_{t+1}).$$

In settings where the state space and/or action space is large enough that the state-action value function $\mathcal{Q}(s, a)$ cannot be held in a tabular form, a function approximator is used. Thus, for deep reinforcement learning the $\mathcal{Q}$-function is approximated via deep neural networks.

$$\theta_{t+1} = \theta_t + \alpha(\mathcal{R}(s_t, a_t, s_{t+1}) + \gamma \mathcal{Q}(s_{t+1}, \arg\max_a \mathcal{Q}(s_{t+1}, a; \theta_t); \theta_t) - \mathcal{Q}(s_t, a_t; \theta_t)) \nabla_{\theta_t} \mathcal{Q}(s_t, a_t; \theta_t).$$

**Dueling Architecture:** At the end of convolutional layers for a given deep $\mathcal{Q}$-Network, the dueling architecture outputs two streams of fully connected layers for both estimating the state values $\mathcal{V}(s)$ and the advantage $\mathcal{A}(s, a)$ for each action in a given state $s$, $\mathcal{A}(s, a) = \mathcal{Q}(s, a) - \max_a \mathcal{Q}(s, a)$. In particular, the last layer of the dueling architecture contains the forward mapping

$$\mathcal{Q}(s, a; \theta, \alpha, \beta) = \mathcal{V}(s; \theta, \beta) + \left(\mathcal{A}(s, a; \theta, \alpha) - \max_{a' \in A} \mathcal{A}(s, a'; \theta, \alpha)\right) \tag{1}$$

where $\theta$ represents the parameters of the convolutional layers and $\alpha$ and $\beta$ represent the parameters of the fully connected layers outputting the advantage and state value estimates respectively.

**Learning the State-Action Value Distribution:** The initial algorithm proposed to learn the state-action value distribution is C51. The projected Bellman update for the $i^{\text{th}}$ atom is computed as

$$(\Phi \mathcal{T} \mathcal{Z}_\theta(s_t, a_t))_i = \sum_{j}^{\mathcal{N}-1} \left[1 - \frac{|[\mathcal{T} z_j]_{v_{\min}}^{v_{\max}} - z_i|}{\Delta z}\right]_0^1 \tau_j(s_{t+1}, \max_{a \in A} \mathbb{E} \mathcal{Z}_\theta(s_{t+1}, a)) \tag{2}$$

where $\mathcal{Z}_\theta(s_t, a_t)$ is the value distribution, $z_i = v_{\min} + i\Delta z : 0 \le i < \mathcal{N}$ represents the set of atoms in categorical learning, and the atom probabilities are learnt as a parametric model

$$\tau_i(s_t, \max_{a \in A} \mathbb{E} \mathcal{Z}_\theta(s_t, a)) = \frac{e^{\theta_i(s_t, a_t)}}{\sum_j e^{\theta_j(s_t, a_t)}} \;,\; \Delta z := \frac{v_{\max} - v_{\min}}{\mathcal{N} - 1} \tag{3}$$

Following this baseline algorithm the $\mathcal{Q}$RD$\mathcal{Q}$N algorithm is proposed to learn the quantile projection of the state-action value distribution

$$\mathcal{T}\mathcal{Z}(s_t, a_t) = \mathcal{R}(s_t, a_t, s_{t+1}) + \gamma\mathcal{Z}(s_{t+1}, \arg\max_{a\in A} \mathbb{E}_{z\sim\mathcal{Z}(s_{t+1},a_{t+1})}[z]) \tag{4}$$

with $s_{t+1} \sim \mathcal{P}(\cdot|s_t, a_t)$ where $\mathcal{Z} \in Z$ represents the quantile distribution of an arbitrary value function. Following this study the I$\mathcal{Q}$N algorithm is proposed (i.e. implicit quantile networks) to learn the full quantile function instead of learning a discrete set of quantiles as in the $\mathcal{Q}$RD$\mathcal{Q}$N algorithm. The I$\mathcal{Q}$N algorithm objective is to minimize the loss function

$$\mathcal{L} = \frac{1}{\mathcal{K}} \sum_{i=1}^{\mathcal{K}} \sum_{j=1}^{\mathcal{K}'} \rho_\delta(\mathcal{R}(s_t, a_t, s_{t+1}) + \gamma\mathcal{Z}_{\delta_j'}(s_{t+1}, \arg\max_{a\in A} \mathcal{Q}_\beta(s_t, a_t)) - \mathcal{Z}_{\delta_i}(s_t, a_t)) \tag{5}$$

where $\rho_\delta$ represents the Huber quantile regression loss, and $\mathcal{Q}_\beta = \int_0^1 \mathcal{F}_{\mathcal{Z}}^{-1}(\delta)d\beta(\delta)$. Note that $\mathcal{Z}_\delta = \mathcal{F}_{\mathcal{Z}}^{-1}(\delta)$ is the quantile function of the random variable $\mathcal{Z}$ at $\delta \in [0, 1]$.

## 3 Low-data Regime versus Asymptotic Performance

The high-level message of our empirical results is that comparing the asymptotic performance of two reinforcement learning algorithms does not necessarily give useful information on their relative performance in the low-data regime. In this section we provide mathematical motivation for this claim in the setting of optimizing non-stationary policies (i.e. rewards and transitions can vary with each step in an episode) in undiscounted, finite-horizon MDPs with linear function approximation. This is a setting that has seen recent progress in provable regret bounds with function approximation (Zanette et al., 2020). In particular, a finite horizon MDP is represented as a tuple $\langle S, A, \mathcal{P}, \mathcal{R}, \mathcal{H}\rangle$ where $S$ is the set of states, and $A$ represents the set of actions. For each timestep $t \in [\mathcal{H}] = \{1, \ldots, \mathcal{H}\}$, state $s$, and action $a$ the transition probability kernel $\mathcal{P}_t(s_{t+1}|s_t, a_t)$ gives the probability distribution over the next state, and the reward $\mathcal{R}_t(s_t, a_t, s_{t+1})$ gives the immediate rewards. A non-stationary policy $\pi = (\pi_1, \ldots, \pi_{\mathcal{H}})$ induces a state-action value function given by

$$\mathcal{Q}_t^\pi(s_t, a_t) = \mathcal{R}_t(s_t, a_t, s_{t+1}) + \mathbb{E}_{s_t\sim\mathcal{P}_t(s_{t+1}|s_t,a_t), a_t\sim\pi}\left[\sum_{h=t+1}^{\mathcal{H}} \mathcal{R}_t(s_h, \pi_h(s_h), s_{h+1})\middle| s_t, a_t\right] \tag{6}$$

where we let $\pi(s)$ be the action taken by the policy $\pi$ in state $s$, and the corresponding value function $\mathcal{V}_t^\pi(s_t) = \mathcal{Q}_t(s_t, \pi(s_t))$. The optimal non-stationary policy $\pi^*$ has value function $\mathcal{V}_t^*(s_t) = \mathcal{V}_t^{\pi^*}(s_t)$ satisfying $\mathcal{V}_t^*(s_t) = \sup_\pi \mathcal{V}_t^\pi(s_t)$. The objective is to learn a sequence of non-stationary policies $\pi^k$ for $k \in \{1, \ldots, \mathcal{K}\}$ while interacting with an unknown MDP in order to minimize the regret, which is measured asymptotically over $\mathcal{K}$ episodes of length $\mathcal{H}$

$$\textsc{Regret}(\mathcal{K}) = \sum_{k=1}^{\mathcal{K}} \left(\mathcal{V}_1^*(s_1^k) - \mathcal{V}_1^{\pi^k}(s_1^k)\right) \tag{7}$$

where $s_1^k \in S$ is the starting state of the $k$-th episode. In words, regret sums up the gap between the expected rewards obtained by the sequence of learned policies $\pi^k$ and those obtained by $\pi^*$ when learning for $\mathcal{K}$ episodes. In the linear function approximation setting there is a feature map $\phi_t : S \times A \to \mathbb{R}^{d_t}$ for each $t \in [\mathcal{H}]$ that sends a state-action pair $(s, a)$ to the $d_t$-dimensional vector $\phi_t(s, a)$. Then, the state-action value function $\mathcal{Q}_t(s_t, a_t)$ is parameterized by a vector $\theta_t \in \mathbb{R}^{d_t}$ so that $\mathcal{Q}_t(\theta_t)(s_t, a_t) = \phi_t(s, a)^\top\theta_t$. Recent theoretical work in this setting gives an algorithm along with a lower bound that matches the regret achieved by the algorithm up to logarithmic factors.

**Theorem 3.1** (Zanette et al. (2020)). *Under appropriate normalization assumptions there is an algorithm that learns a sequence of policies $\pi^k$ achieving regret*

$$\textsc{Regret}(\mathcal{K}) = \tilde{O}\left(\sum_{t=1}^{\mathcal{H}} d_t\sqrt{\mathcal{K}} + \sum_{t=1}^{\mathcal{H}} \sqrt{d_t}\mathcal{I}\mathcal{K}\right), \tag{8}$$

*where $\mathcal{I}$ is the intrinsic Bellman error. Furthermore, this regret bound is optimal for this setting up to logarithmic factors in $d_t, \mathcal{K}$ and $\mathcal{H}$ whenever $\mathcal{K} = \Omega((\sum_{t=1}^{\mathcal{H}} d_t)^2)$, in the sense that for any level of intrinsic Bellman error $\mathcal{I}$ and sequence of feature dimensions $\{d_t\}_{t=1}^H$, there exists a class of MDPs $\mathcal{C}(\mathcal{I}, \{d_t\}_{t=1}^H)$ where any algorithm achieves at least as much regret on at least one MDP in the class.*

The class of MDPs $\mathcal{C}(\mathcal{I}, \{d_t\}_{t=1}^H)$ constructed in Theorem 3.1 additionally satisfies the following properties. First, every MDP in $\cup_{\mathcal{I},\{d_t\}_{t=1}^H}\mathcal{C}(\mathcal{I}, \{d_t\}_{t=1}^H)$ has the same transitions (up to renaming of states and actions). Second, for each fixed value of the intrinsic Bellman error $\mathcal{I}$ and the dimensions $\{d_t\}_{t=1}^H$, every MDP in $\mathcal{C}(\mathcal{I}, \{d_t\}_{t=1}^H)$ utilizes the same feature map $\phi_t(s_t, a_t)$. Thus one can view the class $\mathcal{C}(\mathcal{I}, \{d_t\}_{t=1}^H)$ as encoding one "underlying" true environment (defined by the transitions), with varying values of $\mathcal{I}$ and $\{d_t\}_{t=1}^H$ corresponding to varying levels of function approximation accuracy, and model capacity for the underlying environment. For simplicity of notation we will focus on the setting where $d_t = d$ for all $t \in \{1, \dots H\}$ and write $\mathcal{C}(\mathcal{I}, d)$ for the class of MDPs constructed in Theorem 3.1 for this setting. Utilizing this point of view, we can then prove the following proposition on the relationship between the performance in the asymptotic and low-data regimes.

**Theorem 3.2.** *For any $\epsilon > 0$, let $d_\alpha$ be any feature dimension, and let $d_\beta = d_\alpha^{1-\epsilon/2}$. Then there exist thresholds $\mathcal{K}_{low} < \mathcal{K}_{high}$ and intrinsic Bellman error levels $\mathcal{I}_\beta > \mathcal{I}_\alpha$ such that*

1. *There is an algorithm achieving regret $\text{REGRET}_{low}(\mathcal{K})$ when $\mathcal{K} < \mathcal{K}_{low}$ for all MDPs in $\mathcal{C}(\mathcal{I}_\beta, d_\beta)$. However, every algorithm has regret at least $\widetilde{\Omega}\left(d_\beta^{\epsilon/2}\text{REGRET}_{low}(\mathcal{K})\right)$ when $\mathcal{K} < \mathcal{K}_{low}$ on some MDP $M \in \mathcal{C}(\mathcal{I}_\alpha, d_\alpha)$.*
2. *There is an algorithm achieving regret $\text{REGRET}_{high}(\mathcal{K})$ when $\mathcal{K} > \mathcal{K}_{high}$ for all MDPs in $\mathcal{C}(\mathcal{I}_\alpha, d_\alpha)$. However, every algorithm has regret at least $\widetilde{\Omega}\left(d_\alpha^{\epsilon}\text{REGRET}_{high}(\mathcal{K})\right)$ on some MDP $M \in \mathcal{C}(\mathcal{I}_\beta, d_\beta)$ when $\mathcal{K} > \mathcal{K}_{high}$.*

*Proof.* Let $\epsilon > 0$ and consider $d_\beta = d_\alpha^{1-\frac{\epsilon}{2}}, \mathcal{I}_\beta = \frac{1}{d_\alpha^\epsilon\sqrt{d_\beta}}, \mathcal{I}_\alpha = \frac{1}{d_\alpha^{\frac{1}{2}+2\epsilon}}, \mathcal{K}_{\text{low}} = d_\alpha^{2+\epsilon}, \mathcal{K}_{\text{high}} = d_\alpha^{2+4\epsilon}$ We begin with the proof of part 1. Therefore, for $\mathcal{K} < \mathcal{K}_{\text{low}}$,

$$\sqrt{d_\beta}\mathcal{I}_\beta\mathcal{K} = d_\alpha^{-\epsilon}\mathcal{K} < d_\alpha^{1-\frac{\epsilon}{2}}\sqrt{\mathcal{K}} = d_\beta\sqrt{\mathcal{K}}. \tag{9}$$

Therefore, by Theorem 3.1 there exists an algorithm achieving regret

$$\text{REGRET}_{\text{low}}(\mathcal{K}) = \tilde{O}\left(\mathcal{H}d_\beta\sqrt{\mathcal{K}} + \mathcal{H}\sqrt{d_\beta}\mathcal{I}_\beta\mathcal{K}\right) = \tilde{O}\left(d_\beta\sqrt{\mathcal{K}}\right) \tag{10}$$

in every MDP $M \in \mathcal{C}(\mathcal{I}_\beta, d_\beta)$. Further, since $\mathcal{K}_{\text{low}} = d_\alpha^{2+\epsilon} > \widetilde{\Omega}\left(d_\alpha^2\right)$, the lower bound from Theorem 3.1 applies to the class of MDPs $\mathcal{C}(\mathcal{I}_\alpha, d_\alpha)$ for all $\mathcal{K} \in \left[\widetilde{\Omega}\left(d_\alpha^2\right), \mathcal{K}_{\text{low}}\right]$. In particular, every algorithm receives regret at least

$$\begin{aligned}\text{REGRET}(\mathcal{K}) = \widetilde{\Omega}\left(\mathcal{H}d_\alpha\sqrt{\mathcal{K}} + \mathcal{H}\sqrt{d_\alpha}\mathcal{I}_\alpha\mathcal{K}\right) > \widetilde{\Omega}\left(\mathcal{H}d_\beta^{\frac{1}{1-\epsilon/2}}\sqrt{\mathcal{K}}\right) > \widetilde{\Omega}\left(\mathcal{H}d_\beta^{\frac{\epsilon/2}{1-\epsilon/2}}d_\beta\sqrt{\mathcal{K}}\right)\\ > \widetilde{\Omega}\left(d_\beta^{\epsilon/2}\text{REGRET}_{\text{low}}(\mathcal{K})\right).\end{aligned}$$

For part 2, note that for $\mathcal{K} > \mathcal{K}_{\text{high}}$ we have both

$$\sqrt{d_\alpha}\mathcal{I}_\alpha\mathcal{K} = d_\alpha^{-2\epsilon}\mathcal{K} > d_\alpha^{-2\epsilon}\sqrt{\mathcal{K}\cdot\mathcal{K}_{\text{high}}} > d_\alpha\sqrt{\mathcal{K}}$$

and

$$\sqrt{d_\beta}\mathcal{I}_\beta\mathcal{K} > d_\alpha^{-\epsilon}\sqrt{\mathcal{K}\cdot\mathcal{K}_{\text{low}}} = d_\alpha^{1+\epsilon}\sqrt{\mathcal{K}} > d_\beta\sqrt{\mathcal{K}}.$$

Therefore again by Theorem 3.1 that for $\mathcal{K} > \mathcal{K}_{\text{low}}$ there exists an algorithm achieving regret

$$\text{REGRET}_{\text{high}}(\mathcal{K}) = \tilde{O}\left(\mathcal{H}d_\alpha\sqrt{\mathcal{K}} + \mathcal{H}\sqrt{d_\alpha}\mathcal{I}_\alpha\mathcal{K}\right) = \tilde{O}\left(\mathcal{H}\sqrt{d_\alpha}\mathcal{I}_\alpha\mathcal{K}\right). \tag{11}$$

for every MDP $M \in \mathcal{C}(\mathcal{I}_\alpha, d_\alpha)$. However, by the lower bound in Theorem 3.1, for $\mathcal{K} > \mathcal{K}_{\text{low}}$ every algorithm receives regret at least

$$\begin{aligned}\text{REGRET}(\mathcal{K}) &= \widetilde{\Omega}\left(\mathcal{H}d_\beta\sqrt{\mathcal{K}} + \mathcal{H}\sqrt{d_\beta}\mathcal{I}_\beta\mathcal{K}\right) > \widetilde{\Omega}\left(\mathcal{H}\sqrt{d_\beta}\mathcal{I}_\beta\mathcal{K}\right)\\ &= \widetilde{\Omega}\left(\mathcal{H}d_\alpha^{-\epsilon}\mathcal{K}\right) = \widetilde{\Omega}\left(d_\alpha^{\epsilon}\mathcal{H}d_\alpha^{-2\epsilon}\mathcal{K}\right) = \widetilde{\Omega}\left(d_\alpha^{\epsilon}\mathcal{H}\sqrt{d_\alpha}\mathcal{I}_\alpha\mathcal{K}\right)\\ &> \widetilde{\Omega}\left(d_\alpha^{\epsilon}\text{REGRET}_{\text{high}}(\mathcal{K})\right)\end{aligned}$$

□

Theorem 3.2 shows that in the linear function approximation setting, there is a provable trade-off between performance in the low-data regime (i.e. $\mathcal{K} < \mathcal{K}_{\text{low}}$) and the high-data regime (i.e. $\mathcal{K} > \mathcal{K}_{\text{high}}$). In particular, in the low-data regime lower capacity function approximation (lower feature dimension $d_\beta$) with larger approximation error (larger intrinsic Bellman error $\mathcal{I}_\beta$) can provably outperform larger capacity models (feature dimension $d_\alpha$) with smaller approximation error (intrinsic Bellman error $\mathcal{I}_\alpha$). Furthermore, the relative performance is reversed in the high-data regime $\mathcal{K} > \mathcal{K}_{\text{high}}$. Thus, comparisons between algorithms in the asymptotic/high-data regime are not informative when trying to understand algorithm performance with limited data.

## 4 Lower Bounds for Learning the State-Action Value Distribution

The instances of the implicit assumption that the performance profile of an algorithm in the high-data regime will translate to the low-data regime monotonically appear in almost all of the studies conducted in the low-data regime. In particular, we see that when this line of work was being conducted the best performing algorithm in the high-data regime was based on learning the state action value distribution. Hence, there are many cases in the literature (e.g. DRQ, OTR, DER, CURL, SimPLE, Efficient-Zero) where all the newly proposed algorithms in the low-data regime are being compared to an algorithm that learns the state-action value distribution, under the implicit assumption that the algorithm that learns the state-action value distribution must achieve the current best performance in the low-data regime. The large scale experiments provided in Section 5 demonstrate the impact of this implicit assumption in the low-data regime deep reinforcement learning algorithm design. In particular, the results reported in Section 5 prove that the performance profile of an algorithm in the high-data regime does not monotonically transfer to the low-data regime. Due to this extensive focus throughout the literature on low-data regime comparisons to algorithms that learn the state action value distribution, we provide additional theoretical justification for the empirically observed sample complexity results in the low to high-data regime in deep reinforcement learning.

To obtain theoretical insight into the larger sample complexity exhibited by learning the state-action value distribution we consider the fundamental comparison between learning the distribution of a random variable $\mathcal{X}$ versus only learning the mean $\mathbb{E}[\mathcal{X}]$. In the base algorithm that learns the state-action value distribution the goal is to learn a distribution over state-action values that has finite support. It is well-known that learning a discrete distribution to error $\epsilon$ in total variation distance requires more samples than estimating the mean to within error epsilon (see Proposition A.1). Although this fact implies that learning the state-action value distribution has an intrinsically higher sample complexity than that of standard $\mathcal{Q}$-learning, it does not provide insights into the comparison of an error of $\epsilon$ in the mean with an error of $\epsilon$ in total variation distance. Hence, the following proposition demonstrates a precise justification of the comparison: whenever there are two different actions where the true mean state-action values are within $\epsilon$, an approximation error of $\epsilon$ in total variation distance for the state-action value distribution of one of the actions is sufficient to reverse the order of the means.

**Proposition 4.1.** *Fix a state $s$ and consider two actions $a, a'$. Let $\mathcal{X}(s,a)$ be the random variable distributed as the true state-action value distribution of $(s,a)$, and $\mathcal{X}(s,a')$ be the same for $(s,a')$. Suppose that $\mathbb{E}[\mathcal{X}(s,a)] = \mathbb{E}[\mathcal{X}(s,a')] + \epsilon$. Then there is a random variable $\mathcal{Y}$ such that $d_{TV}(\mathcal{Y}, \mathcal{X}(s,a)) \leq \epsilon$ and $\mathbb{E}[\mathcal{X}(s,a')] \geq \mathbb{E}[\mathcal{Y}]$.*

*Proof.* Let $\tau^* \in \mathbb{R}$ be the infimum $\tau^* = \inf\{\tau \in \mathbb{R} \mid \mathbb{P}[\mathcal{X}(s,a) \geq \tau] = \epsilon\}$ i.e. $\tau^*$ is the first point in $\mathbb{R}$ such that $\mathcal{X}(s,a)$ takes values at least $\tau^*$ with probability exactly $\epsilon$. Next let the random variable $\mathcal{Y}$ be defined by the following process. First, sample the random variable $\mathcal{X}(s,a)$. If $\mathcal{X}(s,a) \geq \tau^*$, then output $\tau^* - 1$. Otherwise, output the sampled value of $\mathcal{X}(s,a)$. Observe that the probability distributions of $\mathcal{Y}$ and $\mathcal{X}(s,a)$ are identical except at the point $\tau^* - 1$ and on the interval $[\tau^*, \infty)$. Let $\mu$ be the Lebesgue measure on $\mathbb{R}$. By construction of $\mathcal{Y}$ the total variation distance is given by

$$d_{TV}(\mathcal{Y}, \mathcal{X}) = \frac{1}{2}\int_{\mathbb{R}} \big|\mathbb{P}[\mathcal{X}(s,a) = z] - \mathbb{P}[\mathcal{Y} = z]\big|\, d\mu(z) = \frac{1}{2}\big|\mathbb{P}[\mathcal{X}(s,a) = \tau^* - 1] - \mathbb{P}[\mathcal{Y} = \tau^* - 1]\big| + \frac{1}{2}\int_{[\tau^*,\infty)} \big|\mathbb{P}[\mathcal{X}(s,a) = z] - \mathbb{P}[\mathcal{Y} = z]\big|\, d\mu(z) = \frac{\epsilon}{2} + \frac{\epsilon}{2} = \epsilon.$$

Next note that the expectation of $\mathcal{Y}$ is given by

$$\begin{aligned}\mathbb{E}[\mathcal{Y}] &= \epsilon(\tau^* - 1) + \int_{(-\infty,\tau^*]} z\mathbb{P}[\mathcal{X}(s,a) = z]\, d\mu(z) \\ &= \epsilon(\tau^* - 1) + \int_{\mathbb{R}} z\mathbb{P}[\mathcal{X}(s,a) = z]\, d\mu(z) - \int_{(\tau^*,\infty]} z\mathbb{P}[\mathcal{X}(s,a) = z]\, d\mu(z) \\ &\leq \epsilon(\tau^* - 1) + \mathbb{E}[\mathcal{X}(s,a)] - \epsilon\tau^* = \mathbb{E}[\mathcal{X}(s,a)] - \epsilon\end{aligned}$$

where the inequality follows from the fact that $\mathcal{X}$ takes values larger than $\tau^*$ with probability $\epsilon$. □

To summarize, Proposition 4.1 shows that, in the case where the mean state-action values are within $\epsilon$, unless the state-action value distribution is learned to within total-variation distance $\epsilon$, the incorrect action may be selected by the policy that learns the state-action value distribution. Therefore, it is natural to compare the sample complexity of learning the state-action value distribution to within total-variation distance $\epsilon$ with the sample complexity of simply learning the mean to within error $\epsilon$, as is done in Proposition A.1.

### 4.1 Sample Complexity with Unknown Support

The setting considered in Proposition A.1 most readily applies to the base algorithm that learns the state-action value distribution C51, which attempts to directly learn a discrete distribution with known support in order to approximate the state-action value distribution. However, further advances in learning the state-action value distribution including $\mathcal{Q}$RD$\mathcal{Q}$N and I$\mathcal{Q}$N do away with the assumption that the support of the distribution is known. This allows a more flexible representation in order to more accurately represent the true distribution on state-action values, but, as we will show, potentially leads to a further increase in the sample complexity. The $\mathcal{Q}$RD$\mathcal{Q}$N algorithm models the distribution of state-action values as a uniform mixture of $\mathcal{N}$ Dirac deltas on the reals i.e. $\mathcal{Z}(s,a) = \frac{1}{\mathcal{N}} \sum_{i=1}^{\mathcal{N}} \delta_{\theta_i(s,a)}$, where $\theta_i(s,a) \in \mathbb{R}$ is a parametric model.

**Proposition 4.2.** *Let $\mathcal{N} > \mathcal{M} \geq 2$, $\epsilon > \frac{\mathcal{M}}{4\mathcal{N}}$, and $\theta_i \in \mathbb{R}$ for $i \in [\mathcal{N}]$. The number of samples required to learn a distribution of the form $\mathcal{Z} = \frac{1}{\mathcal{N}} \sum_{i=1}^{\mathcal{N}} \delta_{\theta_i}$ to within total variation distance $\epsilon$ is $\Omega\left(\frac{\mathcal{M}}{\epsilon^2}\right)$.*

The proof is provided in the appendix. Depending on the choice of parameters, the lower bound in Proposition 4.2 can be significantly larger than that of Proposition A.1. For example if the desired approximation error is $\epsilon = \frac{1}{8}$ one can take $\mathcal{M} = \frac{\mathcal{N}}{2}$. In this case if the value of $k$ in Proposition A.1 satisfies $k = o(\mathcal{N})$, then the sample complexity in Proposition 4.2 is asymptotically larger than that of Proposition A.1.

## 5 Large Scale Experimental Investigation

The experiments are conducted in the Arcade Learning Environment (ALE) (Bellemare et al., 2013). The Double $\mathcal{Q}$-learning algorithm is trained via Double Deep $\mathcal{Q}$-Network (Hasselt et al., 2016a) initially proposed by van Hasselt (2010). The dueling algorithm is trained via Wang et al. (2016). The prior algorithm refers to the prioritized experience replay algorithm proposed by Schaul et al. (2016). The policies that learn the state-action value distribution are trained via the C51 algorithm, I$\mathcal{Q}$N and $\mathcal{Q}$RD$\mathcal{Q}$N. To provide a complete picture of the sample complexity we conducted our experiments in both low-data, i.e. the Arcade Learning Environment 100K benchmark, and high data regime, i.e. baseline 200 million frame training. All of the results are reported with the standard error of the mean in all of the tables and figures in the paper. The experiments are run with JAX (Bradbury et al., 2018), with Haiku as the neural network library, Optax (Hessel et al., 2020) as the optimization library, and RLax for the reinforcement learning library (Babuschkin et al., 2020). More details on the hyperparameters and direct references to the implementations can be found in the supplementary material. Note that human normalized score is computed as follows:

$$\text{Score}_{\text{HN}} = \frac{\text{Score}_{agent} - \text{Score}_{random}}{\text{Score}_{human} - \text{Score}_{random}}$$

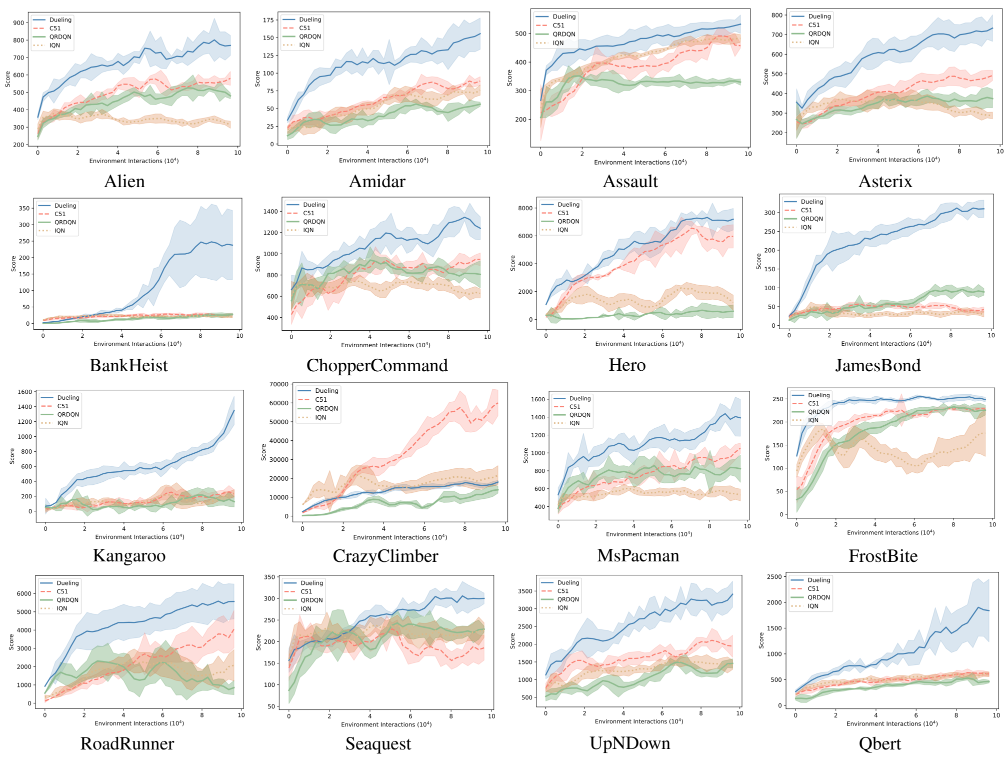

Figure 1: The learning curves of Alien, Amidar, Asterix, BankHeist, ChopperCommand, Hero, CrazyClimber, JamesBond, Kangaroo, MsPacman, FrostBite, Qbert, RoadRunner, Seaquest and UpNDown with dueling architecture, C51, I$\mathcal{Q}$N and $\mathcal{Q}$RD$\mathcal{Q}$N algorithms in the Arcade Learning Environment with 100K environment interaction training.

Figure 1 reports learning curves for the I$\mathcal{Q}$N, $\mathcal{Q}$RD$\mathcal{Q}$N, dueling architecture and C51 for every MDP in the Arcade Learning Environment low-data regime 100K benchmark. These results demonstrate that the simple base algorithm dueling performs significantly better than any algorithm that focuses on learning the distribution when the training samples are limited. For a fair, direct and transparent comparison we kept the hyperparameters for the baseline algorithms in the low-data regime exactly the same with the DR$\mathcal{Q}^{\text{ICLR}}$ paper (see supplementary material for the full list and high-data regime hyperparameter settings). Note that the DR$\mathcal{Q}$ algorithm uses the dueling architecture without any distributional reinforcement learning. One intriguing takeaway from the results provided in Table 1 and the Figure 4[1] is the fact that the simple base algorithm dueling performs 15% better than the DR$\mathcal{Q}^{\text{NeurIPS}}$ implementation, and 11% less than the DR$\mathcal{Q}^{\text{ICLR}}$ implementation. Note that the original paper of the DR$\mathcal{Q}^{\text{ICLR}}$ algorithm provides comparison only to data-efficient Rainbow (DER) (van Hasselt et al., 2019) which inherently learns the state-action value distribution. The fact that the original paper that proposed data augmentation for deep reinforcement learning (i.e. DR$\mathcal{Q}^{\text{ICLR}}$) on top of the dueling architecture did not provide comparisons with the pure simple base dueling architecture (Wang et al., 2016) resulted in inflated performance profiles for the DR$\mathcal{Q}^{\text{ICLR}}$ algorithm.

More intriguingly, the comparisons provided in the DR$\mathcal{Q}^{\text{ICLR}}$ paper to the DER and OTR algorithms report the performance gained by DR$\mathcal{Q}^{\text{ICLR}}$ over DER is 82% and over OTR is 35%. However, if a direct comparison is made to the simple dueling algorithm as Table 1 demonstrates with the exact hyperparameters used as in the DR$\mathcal{Q}^{\text{ICLR}}$ paper the performance gain is utterly restricted to **11%**. Moreover, when it is compared to the reproduced results of DR$\mathcal{Q}^{\text{NeurIPS}}$ it turns out that there is a performance decrease due to utilizing the DR$\mathcal{Q}$ algorithm over dueling architecture. Thus, the fact that our paper provides foundations on the non-monotonicity of the performance profiles from

[1]DER$^{2021}$ refers to the re-implementation with random seed variations of the original paper data-efficient Rainbow (i.e. DER$^{2019}$) by van Hasselt et al. (2019). OTR refers to further implementation of the Rainbow algorithm by Kielak (2019). DR$\mathcal{Q}^{\text{NeurIPS}}$ refers to the re-implementation of the original DR$\mathcal{Q}$ algorithm published in ICLR as a spotlight presentation with the goal of achieving reproducibility with variation on the number of random seeds (Agarwal et al., 2021).

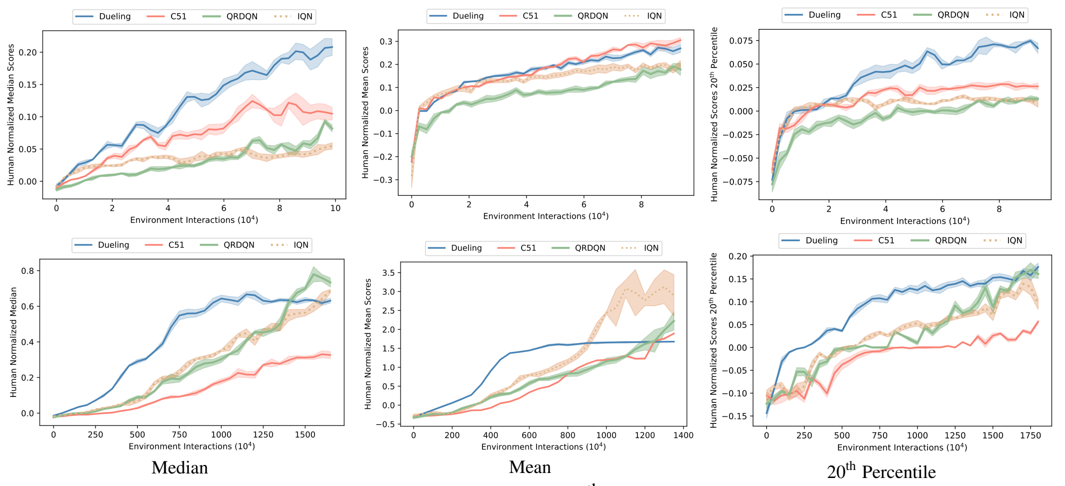

Figure 2: Up: Human normalized median, mean and 20th percentile results for the dueling algorithm, C51, I$\mathcal{Q}$N and $\mathcal{Q}$RD$\mathcal{Q}$N in the Arcade Learning Environment 100K benchmark. Down: Human normalized median, mean, and 20th percentile results for the dueling algorithm, C51, I$\mathcal{Q}$N and $\mathcal{Q}$RD$\mathcal{Q}$N in the high-data regime towards 200 million frame.

Table 1: Large scale comparison of $\mathcal{Q}$-based deep reinforcement learning algorithms with human normalized mean, median and 20th percentile results in the Arcade Learning Environment 100K benchmark for D$\mathcal{Q}$N (Mnih et al., 2015), deep Double-$\mathcal{Q}$ learning (Hasselt et al., 2016a), dueling architecture (Wang et al., 2016), Prior (Schaul et al., 2016), C51, $\mathcal{Q}$RD$\mathcal{Q}$N and I$\mathcal{Q}$N.

| Algorithms | Human Normalized Median | Human Normalized Mean | 20th Percentile |
|---|---|---|---|
| D$\mathcal{Q}$N | 0.0481±0.0036 | 0.1535±0.0119 | 0.0031±0.0032 |
| Double-$\mathcal{Q}$ | 0.0920±0.0181 | **0.3169±0.0196** | 0.0341±0.0042 |
| Dueling | **0.2304±0.0061** | 0.2923±0.0060 | **0.0764±0.0037** |
| C51 | 0.0941±0.0081 | 0.3106±0.0199 | 0.0274±0.0024 |
| $\mathcal{Q}$RD$\mathcal{Q}$N | 0.0820±0.0037 | 0.2171±0.0098 | 0.0189±0.0031 |
| I$\mathcal{Q}$N | 0.0528±0.0058 | 0.2050±0.0123 | 0.0091±0.0011 |
| Prior | 0.0840±0.0018 | 0.2792±0.0123 | 0.0267±0.0042 |

large-data regime to low-data regime can influence future research to have more concrete and accurate performance profiles for algorithm development in the low-data regime. Table 1 reports the human normalized median, human normalized mean, and human normalized 20th percentile results over all of the MDPs from the 100K Arcade Learning Environment benchmark for D$\mathcal{Q}$N, Double-$\mathcal{Q}$, dueling, C51, $\mathcal{Q}$RD$\mathcal{Q}$N, I$\mathcal{Q}$N and prior. One important takeaway from the results reported in the Table 1 is the fact that one particular algorithm performance profile in 200 million frame training will not directly transfer to the low-data region. Figure 2 reports the learning curves of human normalized median, human normalized mean and human normalized 20th percentile for the dueling algorithm, C51, $\mathcal{Q}$RD$\mathcal{Q}$N, and I$\mathcal{Q}$N in the low-data region. These results once more demonstrate that the performance profile of the simple base algorithm dueling is significantly better than any other algorithm that learns the state-action value distribution when the number of environment interactions are limited.

The left and center plots of Figure 3 report regret curves corresponding to the theoretical analysis in Theorem 3.2 for various choices of the feature dimensionality $d$ and the intrinsic Bellman error $\mathcal{I}$. In particular, the left plot shows the low-data regime where the number of episodes $\mathcal{K} < 1000$, while the right plot shows the high-data regime where $\mathcal{K}$ is as large as $500000$. Notably, the relative ordering of the regret across the different choices of $d$ and $\mathcal{I}$ is completely reversed in the high-data regime when compared to the low-data regime. Recall from Theorem 3.1 that the intrinsic Bellman error is a measure of the accuracy of function approximation under the Bellman operator corresponding to an MDP. Thus, the varying values of $\mathcal{I}$ and $d$ in Figure 3 correspond to a natural setting where increasing the number of model parameters (i.e. increasing $d$) corresponds to an increase in the accuracy of function approximation (i.e. a decrease in $\mathcal{I}$). Thus the results reported in Figure 3 demonstrate that, even in the natural setting where increased model capacity leads to increased accuracy, there can be a complete reversal in the ordering of algorithm performance between the low and high-data regimes.

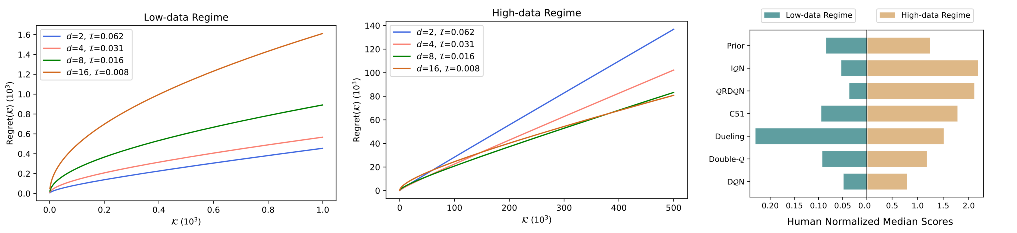

Regret in the Low-data Regime Regret in the High-data Regime Distributional vs Baseline $\mathcal{Q}$

Figure 3: Left: Regret in the low-data regime. Center: Regret in the high-data regime. Right: Distributional vs baseline $\mathcal{Q}$ comparison of algorithms that were proposed and developed in the high-data regime in the Arcade Learning Environment in both high-data regime and low-data regime.

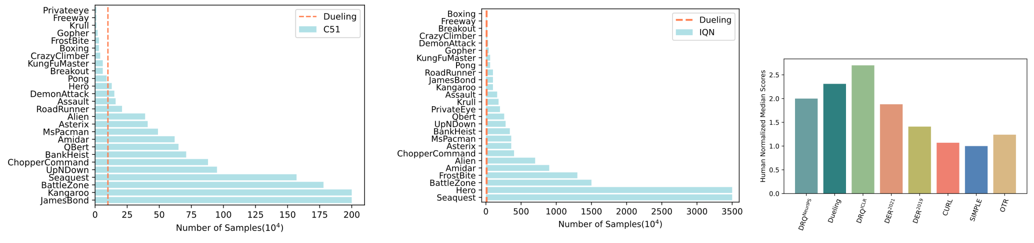

Sample Complexity of C51 Sample Complexity of I$\mathcal{Q}$N Overall Comparison

Figure 4: Left: Number of samples (i.e. environment interactions) required by the base algorithm that learns the state-action value distribution to achieve the performance level achieved by the dueling algorithm. Center: Number of samples required by I$\mathcal{Q}$N to achieve the performance level achieved by dueling. Right: Overall comparison of algorithms recently developed in the low-data regime ALE 100K benchmark to the dueling algorithm that was designed in the high-data region.

Figure 4 reports results on the number of samples required for training with the baseline algorithm that learns the state-action value distribution to reach the same performance levels achieved by the dueling algorithm for each individual MDP from ALE low-data regime benchmark. These results once more demonstrate that to reach the same performance levels with the dueling algorithm, the baseline algorithm that learns the state-action value distribution requires orders of magnitude more samples to train on. As discussed in Section 4.1, more complex representations for broader classes of distributions come at the cost of a higher sample complexity required for learning. One intriguing fact is that the original SimPLE paper provides a comparison in the low-data regime of their proposed algorithm with the Rainbow algorithm which is essentially an algorithm that is designed in the high-data region by having the implicit assumption that the state-of-the art performance profile must transfer monotonically to the low-data region. These instances of implicit assumptions also occur in DR$\mathcal{Q}^{\text{ICLR}}$, CURL, SPR and Efficient-Zero even when comparisons are made for more advanced algorithms such as MuZero. Note that these implicit assumptions give faulty signals on why and what makes these algorithms work when designed for the low-data regime, and hence affect future research directions while misdirecting research efforts from ideas that could have worked in the algorithm design process.

## 6 Conclusion

In this paper we aimed to answer the following questions: (i) *Do the performance profiles of deep reinforcement learning algorithms designed for certain data regimes translate monotonically to a different sample complexity region?*, and (ii) *What is the underlying theoretical relationship between the performance profiles and sample complexity regimes?* To be able to answer these questions we provide theoretical investigation on the sample complexity of the baseline deep reinforcement learning algorithms. We conduct extensive experiments both in the low-data region 100K Arcade Learning Environment and high-data regime baseline 200 million frame training. Our results demonstrate that the performance profiles of deep reinforcement learning algorithms do not have a monotonic relationship across sample complexity regimes. The underlying premise of the monotonic relationship of the performance characteristics and the sample complexity regions that exists in many recent state-of-the-art studies has been assumed incorrectly. Thus, our results demonstrate that several baseline $\mathcal{Q}$ algorithms are almost as high performing as recent variant algorithms that have been proposed and shown as the state-of-the-art.

## REFERENCES

Rishabh Agarwal, Max Schwarzer, Pablo Samuel Castro, Aaron C. Courville, and Marc G. Bellemare. Deep reinforcement learning at the edge of the statistical precipice. In Marc'Aurelio Ranzato, Alina Beygelzimer, Yann N. Dauphin, Percy Liang, and Jennifer Wortman Vaughan (eds.), *Advances in Neural Information Processing Systems 34: Annual Conference on Neural Information Processing Systems 2021, NeurIPS 2021, December 6-14, 2021, virtual*, pp. 29304–29320, 2021.

Igor Babuschkin, Kate Baumli, Alison Bell, Surya Bhupatiraju, Jake Bruce, Peter Buchlovsky, David Budden, Trevor Cai, Aidan Clark, Ivo Danihelka, Claudio Fantacci, Jonathan Godwin, Chris Jones, Tom Hennigan, Matteo Hessel, Steven Kapturowski, Thomas Keck, Iurii Kemaev, Michael King, Lena Martens, Hamza Merzic, Vladimir Mikulik, Tamara Norman, John Quan, George Papamakarios, Roman Ring, Francisco Ruiz, Alvaro Sanchez, Rosalia Schneider, Eren Sezener, Stephen Spencer, Srivatsan Srinivasan, Wojciech Stokowiec, and Fabio Viola. The DeepMind JAX Ecosystem, 2020. URL `http://github.com/deepmind`.

Marc G Bellemare, Yavar Naddaf, Joel Veness, and Michael. Bowling. The arcade learning environment: An evaluation platform for general agents. *Journal of Artificial Intelligence Research.*, pp. 253–279, 2013.

James Bradbury, Roy Frostig, Peter Hawkins, Matthew James Johnson, Chris Leary, Dougal Maclaurin, George Necula, Adam Paszke, Jake VanderPlas, Skye Wanderman-Milne, and Qiao Zhang. JAX: composable transformations of Python+NumPy programs, 2018. URL `http://github.com/google/jax`.

Clément L. Canonne. A short note on learning discrete distributions. 2020. URL `http://arxiv.org/abs/2002.11457`. cite arxiv:2002.11457Comment: This is a review article; its intent is not to provide new results, but instead to gather known (and useful) ones, along with their proofs, in a single convenient location.

Hado van Hasselt, Arthur Guez, and David Silver. Deep reinforcement learning with double q-learning. *Association for the Advancement of Artificial Intelligence (AAAI)*, 2016a.

Hado van Hasselt, Arthur Guez, and David Silver. Deep reinforcement learning with double q-learning. *In Thirtieth AAAI conference on artificial intelligence*, 2016b.

Matteo Hessel, Joseph Modayil, Hado van Hasselt, Tom Schaul, Georg Ostrovski, Will Dabney, Dan Horgan, Bilal Piot, Mohammad Gheshlaghi Azar, and David Silver. Rainbow: Combining improvements in deep reinforcement learning. In Sheila A. McIlraith and Kilian Q. Weinberger (eds.), *Proceedings of the Thirty-Second AAAI Conference on Artificial Intelligence, (AAAI-18), the 30th innovative Applications of Artificial Intelligence (IAAI-18), and the 8th AAAI Symposium on Educational Advances in Artificial Intelligence (EAAI-18), New Orleans, Louisiana, USA, February 2-7, 2018*, pp. 3215–3222. AAAI Press, 2018.

Matteo Hessel, David Budden, Fabio Viola, Mihaela Rosca, Eren Sezener, and Tom Hennigan. Optax: composable gradient transformation and optimisation, in jax!, 2020. URL `http://github.com/deepmind/optax`.

Matteo Hessel, Ivo Danihelka, Fabio Viola, Arthur Guez, Simon Schmitt, Laurent Sifre, Theophane Weber, David Silver, and Hado van Hasselt. Muesli: Combining improvements in policy optimization. In Marina Meila and Tong Zhang (eds.), *Proceedings of the 38th International Conference on Machine Learning, ICML 2021, 18-24 July 2021, Virtual Event*, volume 139 of *Proceedings of Machine Learning Research*, pp. 4214–4226. PMLR, 2021.

Lukasz Kaiser, Mohammad Babaeizadeh, Piotr Milos, Blazej Osinski, Roy H. Campbell, Konrad Czechowski, Dumitru Erhan, Chelsea Finn, Piotr Kozakowski, Sergey Levine, Afroz Mohiuddin, Ryan Sepassi, George Tucker, and Henryk Michalewski. Model based reinforcement learni:ng for atari. In *8th International Conference on Learning Representations, ICLR 2020, Addis Ababa, Ethiopia, April 26-30, 2020*. OpenReview.net, 2020.

Kacper Piotr Kielak. Do recent advancements in model-based deep reinforcement learning really improve data efficiency? *CoRR*, 2019.

Volodymyr Mnih, Koray Kavukcuoglu, David Silver, Andrei A Rusu, Joel Veness, arc G Bellemare, Alex Graves, Martin Riedmiller, Andreas Fidjeland, Georg Ostrovski, Stig Petersen, Charles Beattie, Amir Sadik, Antonoglou, Helen King, Dharshan Kumaran, Daan Wierstra, Shane Legg, and Demis Hassabis. Human-level control through deep reinforcement learning. *Nature*, 518: 529–533, 2015.

Tom Schaul, John Quan, Ioannis Antonogloua, and David Silver. Prioritized experience replay. *International Conference on Learning Representations (ICLR)*, 2016.

Hado van Hasselt. Double q-learning. In John D. Lafferty, Christopher K. I. Williams, John Shawe-Taylor, Richard S. Zemel, and Aron Culotta (eds.), *Advances in Neural Information Processing Systems 23: 24th Annual Conference on Neural Information Processing Systems 2010. Proceedings of a meeting held 6-9 December 2010, Vancouver, British Columbia, Canada*, pp. 2613–2621. Curran Associates, Inc., 2010.

Hado van Hasselt, Matteo Hessel, and John Aslanides. When to use parametric models in reinforcement learning? In Hanna M. Wallach, Hugo Larochelle, Alina Beygelzimer, Florence d'Alché-Buc, Emily B. Fox, and Roman Garnett (eds.), *Advances in Neural Information Processing Systems 32: Annual Conference on Neural Information Processing Systems 2019, NeurIPS 2019, December 8-14, 2019, Vancouver, BC, Canada*, pp. 14322–14333, 2019.

Ziyu Wang, Tom Schaul, Matteo Hessel, Hado Van Hasselt, Marc Lanctot, and Nando. De Freitas. Dueling network architectures for deep reinforcement learning. *Internation Conference on Machine Learning ICML.*, pp. 1995–2003, 2016.

Denis Yarats, Ilya Kostrikov, and Rob Fergus. Image augmentation is all you need: Regularizing deep reinforcement learning from pixels. In *9th International Conference on Learning Representations, ICLR 2021, Virtual Event, Austria, May 3-7, 2021*, 2021.

Weirui Ye, Li:u Shaohuai, Thanard Kurutach, Pieter Abbeel, and Yang Gao. Masteri:ng atari games wi:th limited data. In Marc'Aurelio Ranzato, Alina Beygelzimer, Yann N. Dauphin, Percy Liang, and Jennifer Wortman Vaughan (eds.), *Advances in Neural Information Processing Systems 34: Annual Conference on Neural Information Processing Systems 2021, NeurIPS 2021, December 6-14, 2021, virtual*, pp. 25476–25488, 2021.

Andrea Zanette, Alessandro Lazaric, Mykel J. Kochenderfer, and Emma Brunskill. Learning near optimal policies with low inherent bellman error. In *Proceedings of the 37th International Conference on Machine Learning, ICML 2020, 13-18 July 2020, Virtual Event*, volume 119 of *Proceedings of Machine Learning Research*, pp. 10978–10989. PMLR, 2020. URL `http://proceedings.mlr.press/v119/zanette20a.html`.

## A MEAN ESTIMATION VERSUS LEARNING THE DISTRIBUTION

To get a fundamental understanding of the additional cost of learning the state-action value distribution, we compare the sample complexity of learning the distribution of a finitely supported random variable with that of estimating the mean.

**Proposition A.1** (Canonne (2020))**.** *Let $\mathcal{X}$ be a real-valued random variable with support on exactly $k$ known values. Further, assume $|\mathcal{X}| < 1$ and let $\epsilon > 0$. Any algorithm that learns the distribution $\mathbb{P}(\mathcal{X})$ within total variation distance $\epsilon$ requires $\Omega(k/\epsilon^2)$ samples, while there exists an algorithm to estimate $\mathbb{E}[\mathcal{X}]$ to within error $\epsilon$ using only $O(1/\epsilon^2)$ samples.*

*Proof.* Learning a distribution with known discrete support of size $k$ requires $\Omega(k/\epsilon^2)$ samples to achieve total variation distance at most $\epsilon$ with constant probability (Canonne, 2020). On the other hand, let $\mathcal{X}_1, \dots, \mathcal{X}_n$ be independent samples of the random variable $\mathcal{X}$ and consider the sample mean

$$\bar{\mathcal{X}} = \frac{1}{n}\sum_{i=1}^{n} \mathcal{X}_i. \tag{12}$$

The expectation is given by $\mathbb{E}[\bar{\mathcal{X}}] = \mathbb{E}[\mathcal{X}]$ and the variance is $\sigma^2(\bar{\mathcal{X}}) = \frac{1}{n}\sigma^2(\mathcal{X})$. Further, since $|\mathcal{X}| < 1$ we have that $\sigma^2(X) < 1$ and so $\sigma^2(\bar{\mathcal{X}}) \leq \frac{1}{n}$. Hence, by Chebyshev's inequality

$$\mathbb{P}\left[|\bar{\mathcal{X}} - \mathbb{E}[\mathcal{X}]| > \epsilon\right] \leq \frac{1}{\epsilon^2 n}. \tag{13}$$

Thus with $n = O(\frac{1}{\epsilon^2})$ samples, $\bar{\mathcal{X}}$ is within $\epsilon$ of $\mathbb{E}[\mathcal{X}]$ with constant probability. $\square$

## B SAMPLE COMPLEXITY WITH UNKNOWN SUPPORT

**Proposition B.1.** *Let $\mathcal{N} > \mathcal{M} \geq 2$, $\epsilon > \frac{\mathcal{M}}{4\mathcal{N}}$, and $\theta_i \in \mathbb{R}$ for $i \in [\mathcal{N}]$. The number of samples required to learn a distribution of the form $\mathcal{Z} = \frac{1}{\mathcal{N}}\sum_{i=1}^{\mathcal{N}} \delta_{\theta_i}$ to within total variation distance $\epsilon$ is $\Omega\left(\frac{\mathcal{M}}{\epsilon^2}\right)$.*

*Proof.* Let $\mathcal{M} \geq 2$ and $\mathcal{D} = \{1, 2, \cdots, \mathcal{M}\} \subseteq \mathbb{R}$. First we will show that any distribution $p(z)$ supported on $z \in \mathcal{D}$ is within total-variation distance $\frac{k}{4\mathcal{N}}$ of a distribution of a random variable of the form $\mathcal{Z} = \frac{1}{\mathcal{N}}\sum_{i=1}^{\mathcal{N}} \delta_{\theta_i}$ for numbers $\theta_i \in \mathcal{D}$. Indeed we can construct such a distribution as follows. First let $\tilde{p}(z)$ be the rounded distribution obtained by rounding each probability $p(z)$ to the nearest integer multiple of $\frac{1}{\mathcal{N}}$. The total variation distance between $p(z)$ and $\tilde{p}(z)$ is given by

$$\frac{1}{2}\sum_{z=1}^{\mathcal{M}} |p(z) - \tilde{p}(z)| \leq \frac{1}{2}\sum_{z=1}^{\mathcal{M}} \frac{1}{2\mathcal{N}} \leq \frac{\mathcal{M}}{4\mathcal{N}}. \tag{14}$$

Next partition the set of $\theta_i$ into $\mathcal{M}$ groups $\mathcal{G}_1, \mathcal{G}_2, \dots, \mathcal{G}_{\mathcal{M}}$, where group $\mathcal{G}_z$ has size $\mathcal{N}\tilde{p}(z)$ (this size is an integer by construction of $\tilde{p}$). Finally, for each $\theta_i \in \mathcal{G}_z$ assign $\theta_i = z$. Thus for $\mathcal{Z} = \frac{1}{N}\sum_{i=1}^{\mathcal{N}} \delta_{\theta_i}$ we have for each $z \in \mathcal{D}$

$$\mathbb{P}[\mathcal{Z} = z] = \frac{1}{\mathcal{N}}\sum_{i=1}^{\mathcal{N}} \mathbb{1}[\theta_i = z] = \frac{1}{\mathcal{N}}|\mathcal{G}_z| = \tilde{p}(z). \tag{15}$$

Therefore, any distribution $p(z)$ can be approximated to within total variation distance $\frac{\mathcal{M}}{4\mathcal{N}}$ by a distribution $\mathcal{Z}$ of the prescribed form. Thus, by the sample complexity lower bounds for learning a discrete distribution with known support, for any $\epsilon > \frac{\mathcal{M}}{4\mathcal{N}}$ at least $\frac{\mathcal{M}}{\epsilon^2}$ samples are required to learn a distribution of the form $\mathcal{Z} = \frac{1}{\mathcal{N}}\sum_{i=1}^{\mathcal{N}} \delta_{\theta_i}$. $\square$

## C RESULTS ON THE COMPLETE LIST OF GAMES FROM THE ARCADE LEARNING ENVIRONMENT 100K BASELINE

Table 2 reports the average scores obtained by the human player, random player, baseline $\mathcal{Q}$-based algorithm dueling architecture, baseline algorithm C51 that focuses on learning the distribution,

$\mathcal{Q}$RD$\mathcal{Q}$N and I$\mathcal{Q}$N across all the games in the Arcade Learning Environment 100K baseline. These results once more demonstrate that the baseline $\mathcal{Q}$-based algorithm performs significantly better than any algorithm that aims to learn the distribution as has also been explained in detail in Section 5 in the main body of the paper.

Table 2: Average returns for human, random, dueling Wang et al. (2016), C51, $\mathcal{Q}$RD$\mathcal{Q}$N and I$\mathcal{Q}$N across all the games in the Arcade Learning Environment 100K benchmark.

| Games | Human | Random | C51 | $\mathcal{Q}$RD$\mathcal{Q}$N | I$\mathcal{Q}$N | Dueling |
|---|---|---|---|---|---|---|
| Alien | 7127.7 | 227.8 | 547.16 | 509.57 | 330.81 | **705.58** |
| Amidar | 1719.5 | 5.8 | 78.41 | 55.70 | 74.98 | **199.31** |
| Assault | 742.0 | 222.4 | 465.30 | 314.58 | 488.55 | **503.82** |
| Asterix | 8503.3 | 210.0 | 475.90 | 367.32 | 286.26 | **705.16** |
| BankHeist | 753.1 | 14.2 | 22.81 | 21.53 | 18.17 | **243.19** |
| BattleZone | 37187.5 | 2360.0 | 2728.52 | 6238.27 | 3105.70 | **6880.37** |
| Boxing | 12.1 | 0.1 | 9.60 | 2.03 | **12.41** | 1.68 |
| Breakout | 30.5 | 1.7 | 11.35 | **16.50** | 15.09 | 8.28 |
| ChopperCommand | 7387.8 | 811.0 | 831.83 | 752.51 | 629.04 | **1313.90** |
| CrazyClimber | 35829.4 | 10780.5 | **71776.14** | 21366.42 | 22649.44 | 17039.44 |
| DemonAttack | 1971.0 | 152.1 | 789.09 | 198.01 | **1035.17** | 694.42 |
| Freeway | 29.6 | 0.0 | **20.42** | 5.98 | 19.37 | 5.93 |
| FrostBite | 4334.7 | 65.2 | 215.25 | 218.11 | 192.33 | **259.18** |
| Gopher | 2412.5 | 257.6 | **791.83** | 576.19 | 466.81 | 429.85 |
| Hero | 30826.4 | 1027.0 | 7097.42 | 1108.44 | 1322.63 | **8210.53** |
| Jamesbond | 302.8 | 29.0 | 43.85 | 108.71 | 26.23 | **296.46** |
| Kangaroo | 3035.0 | 52.0 | 301.01 | 120.60 | 294.46 | **1914.86** |
| Krull | 2665.5 | 1598.0 | **3744.04** | 2040.50 | 2319.74 | 2867.78 |
| KungFuMaster | 22736.3 | 258.5 | 6877.62 | **11574.02** | 1526.76 | 5367.90 |
| Mspacman | 6951.6 | 307.3 | 917.78 | 749.29 | 533.98 | **1355.21** |
| Pong | 14.6 | -20.7 | **11.17** | -7.49 | -10.86 | -4.20 |
| PrivateEye | 69571.3 | 24.9 | -103.30 | -6.32 | 33.83 | **100.00** |
| Qbert | 13455.0 | 163.9 | 528.30 | 590.05 | 582.72 | **1710.23** |
| RoadRunner | 7845.0 | 11.5 | 3993.34 | 400.59 | 1202.20 | **6031.80** |
| Seaquest | 42054.7 | 68.4 | 163.69 | 183.25 | 213.87 | **351.10** |
| UpNdDown | 11693.2 | 533.4 | 1970.28 | 1622.67 | 1552.27 | **3553.12** |

Figure 5 reports the learning curves of the complete list of the games in the Arcade Learning Environment 100K benchmark; in particular, for Alien, Amidar, Asterix, BankHeist, BattleZone, Boxing, Breakout, ChopperCommand, Hero, CrazyClimber, JamesBond, Kangaroo, PrivateEye, MsPacman, FrostBite, Qbert, RoadRunner, Seaquest, Pong, Gopher, DemonAttack, Krull, and UpNDown with dueling architecture Wang et al. (2016), C51, I$\mathcal{Q}$N and $\mathcal{Q}$RD$\mathcal{Q}$N algorithms with 100K environment interaction training. The learning curves reported in Figure 5 demonstrate that the number of samples required to obtain the performance level achieved via the simple base dueling architecture is significantly higher for any reinforcement learning algorithm that learns the distribution. Note that the baseline reinforcement learning algorithm C51 focuses on learning the distribution represents the state-action value distribution as a discrete probability distribution supported on 51 fixed atoms evenly spaced between a pre-specified minimum and maximum value. In contrast, QR-D$\mathcal{Q}$N represents the value distribution as the uniform distribution over a larger number of atoms with variable positions on the real line. Thus, QR-D$\mathcal{Q}$N is able to more accurately approximate a broader class of state-action value distributions. Finally, I$\mathcal{Q}$N parameterizes the quantile function of the state-action value distribution via a deep neural network, leading to a yet more flexible representation of the state-action value distribution. As discussed in Section 4, more complex representations for broader classes of distributions come at the cost of a higher sample complexity required for learning.

### C.1 Reproducibility and Configuration Details

The hyperparameter settings of all of the algorithms in our paper, double-$\mathcal{Q}$, dueling, $\mathcal{Q}$RD$\mathcal{Q}$N, and I$\mathcal{Q}$N for the high-data region are exactly the same with the original papers that proposed these algorithms in the high-data region. See the hyperparameter settings in Hasselt et al. (2016) for double-$\mathcal{Q}$, Wang et al. (2016) for dueling architecture, Bellemare et al. (2017) for C51, Dabney et al. (2018a) for $\mathcal{Q}$RD$\mathcal{Q}$N, and Dabney et al. (2018b) for I$\mathcal{Q}$N.

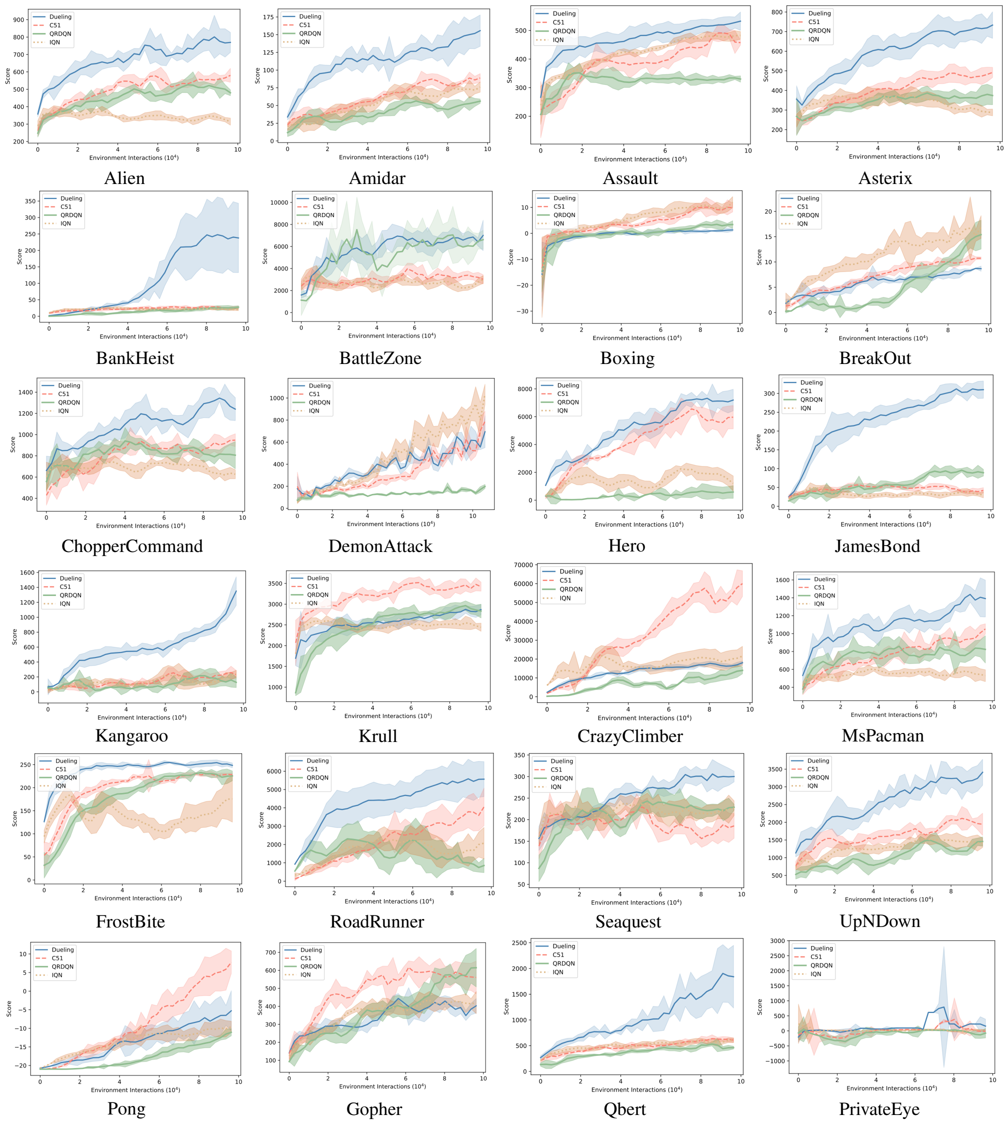

Figure 5: The learning curves of Alien, Amidar, Asterix, BankHeist, BattleZone, Boxing, Breakout, ChopperCommand, Hero, CrazyClimber, JamesBond, Kangaroo, PrivateEye, MsPacman, FrostBite, Qbert, RoadRunner, Seaquest, Pong, Gopher, DemonAttack, Krull, and UpNDown with dueling architecture Wang et al. (2016), C51, I$\mathcal{Q}$N and $\mathcal{Q}$RD$\mathcal{Q}$N algorithms in the Arcade Learning Environment with 100K environment interaction training.

For a fair and transparent comparison, we kept the hyperparameters exactly the same with the DR$\mathcal{Q}^{\text{ICLR}}$ paper for all of the baseline $\mathcal{Q}$ algorithms in the low-data region. Note that DR$\mathcal{Q}$ is an observation regularization study; hence the hyperparameters in the DR$\mathcal{Q}$ paper are specifically tuned for the purpose of the paper besides tuning for the Arcade Learning Environment 100K low-data regime. We did not tune any of the hyperparameters for the baseline algorithms (i.e. dueling architecture). Hence, it is even further possible to conduct hyperparameter tuning and get better performance profile results with the simple baseline dueling architecture. For the purpose of this paper we kept the hyperparameters exactly the same with the DR$\mathcal{Q}^{\text{ICLR}}$ paper. However, we would strongly encourage further research to conduct hyperparameter optimization to obtain better results from the baseline dueling architecture in the low-data regime.

We have also tried the hyperparameter settings reported in the data efficient Rainbow (DER) paper for C51, I$\mathcal{Q}$N and $\mathcal{Q}$RD$\mathcal{Q}$N in the low-data regime. The performance results are provided in Table 4 for

Table 3: Hyperparameter settings and architectural details for the dueling algorithm, double-$\mathcal{Q}$ learning, C51, $\mathcal{Q}$RD$\mathcal{Q}$N, and I$\mathcal{Q}$N in the low-data regime of the Arcade Learning Environment.

| Hyperparameters | Settings |
|---|---|
| Grey-scaling | True |
| Observation down-sampling | (84, 84) |
| Action repetitions | 4 |
| Frames stacked | 4 |
| Batch Size | 32 |
| Update | Double-Q |
| Max Frames per episode | 108000 |
| Evaluation exploration epsilon | 0.01 |
| Min replay size for sampling | 1600 |
| Max gradient norm | 10 |
| Discount factor | 0.99 |
| Maximum absolute rewards | 1 |
| Training steps | 100000 |
| Evaluation steps | 125000 |
| Exploration epsilon decay frame fraction | 0.0125 |
| Gradient error bound | 0.03125 |
| Optimizer | Adam |
| Replay period every | 1 |
| n-step length | 10 |
| Exploration | $\epsilon$-greedy |
| $\epsilon$-decay | 5000 |
| Number of atoms | 51 |
| Number of quantiles | 201 |
| $v_{\max}$ | 10 |
| $\mathcal{Q}$-Network channels | 32,64,64 |
| $\mathcal{Q}$-Network filter size | $8 \times 8, 4 \times 4, 3 \times 3$ |
| $\mathcal{Q}$-Network stride | $(4, 4), (2, 2), (1, 1)$ |
| $\mathcal{Q}$-Network hidden units | 512 |

Table 4: Human normalized mean, human normalized median, and human normalized 20th percentile results for the C51 algorithm, $\mathcal{Q}$RD$\mathcal{Q}$N, and I$\mathcal{Q}$N in the low-data regime of the Arcade Learning Environment with the hyperparameter settings reported in the DER paper.

| Algorithms | Human Normalized Median | Human Normalized Mean | Human Normalized 20th Percentile |
|---|---|---|---|
| C51 | 0.0490±0.0038 | 0.1352±0.0057 | 0.0163±0.0029 |
| $\mathcal{Q}$RD$\mathcal{Q}$N | 0.0203±0.0033 | 0.0778±0.0101 | -0.0012±0.0053 |
| I$\mathcal{Q}$N | 0.0202±0.0020 | 0.0590±0.0139 | -0.0035±0.0031 |

the hyperparameter settings of DER. As can be seen, the hyperparameter settings of DRQ$^{\text{ICLR}}$ gave better performance results also for C51, I$\mathcal{Q}$N and $\mathcal{Q}$RD$\mathcal{Q}$N in the low-data region. The results in Table 4 also align with the claims of the DER paper in which there has not been extensive hyperparameter tuning conducted to achieve the results provided, and it is possible to obtain better results by further hyperparameter tuning.